

SIMPLIFIED MATHEMATICAL MODEL FOR MIGRATION OF GAS BUBBLES IN VISCOPLASTIC FLUIDS

William Lopez

Department of Mechanical Engineering, Pontifícia Universidade Católica do Rio de Janeiro, Rio de Janeiro RJ, Gávea, Rua Marquês de São Vicente, 225, CEP 22451-900.
 wlopez@aluno.puc-rio.br

Mônica Naccache

Department of Mechanical Engineering, Pontifícia Universidade Católica do Rio de Janeiro, Rio de Janeiro RJ, Gávea, Rua Marquês de São Vicente, 225, CEP 22451-900.
 naccache@puc-rio.br

Abstract. *In this work, a study of the rising movement of a single gas bubble in non-Newtonian fluid is performed, in order to simulate the behavior of a gas bubble in a cement paste during oil well cementing. The fluid is modeled as a Herschel-bulkley non-Newtonian fluid, with varying rheology in the time. The same methodology can also be used to simulate the flow of liquid or solid particles. The solution is obtained numerically and the results are compared with experimental results from the literature. The calculations are performed for spherical bubbles, low Reynolds number ($Re < 1$), constant temperature, and neglecting wall effects. The effects of bubble mass and surface tension are analyzed.*

Keywords: *gas bubble, viscoplastic fluid, bubble migration*

7. INTRODUCTION

The study of gas bubble behavior in viscoplastic fluids is of great interest to the industry. In the oil industry, gas bubbles may invade the well during the cementing and cannonade processes. Knowledge of the behavior of gas bubble dynamics inside the cement paste allows a better planning and control of these processes. Therefore, a simplified model providing reliable and fast results, can be very useful to optimize the processes.

1. SIMPLIFIED MATHEMATICAL MODEL.

The kinematics of the bubble inside a fluid, driven by buoyancy, is obtained with a force balance at the bubble (Fig. 1). Following the procedure described in Pinto et al. (2011):

$$\sum F = F_b - F_w + F_d = m \frac{\partial^2 h}{\partial t^2} = ma \quad (1)$$

Where F_b [N] is the buoyancy force, F_d [N] is the drag force, F_w is the bubble weight, a [m/s^2] is the bubble acceleration, m [kg] is the bubble mass, h is the bubble depth and t is time.

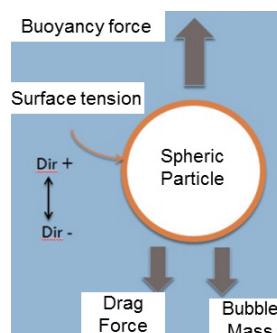


Figure 1. Force balance at the bubble

To calculate the buoyancy force F_b [N], the Archimedes equation is used, where ρ_c [kg/m^3] is the continuous phase density:

$$F_b = \frac{\rho_c g \pi d^3}{6} \quad (2)$$

W. Lopez and M. Naccache
Simplified Mathematical Model for Migration of Gas Bubbles in Viscoplastic.

The bubble weight F_w [N] and the bubble mass are given by:

$$F_w = \frac{\rho_d g \pi d^3}{6} \quad m = \frac{\rho_d \pi d^3}{6} \quad (3)$$

Where ρ_d [kg/m³] is the density of the discrete phase. The drag force F_d [N] is defined by:

$$F_d = \frac{1}{8} \rho_c v^2 \pi d^2 C_D \quad (4)$$

To calculate the drag coefficient C_D we use the model postulated by Ansley and Smith (1967) for Newtonian, Power-Law, Bingham and Herschel-Bulkley fluids, where Re_{pl} is the Generalized Reynolds number, Bi_{hb} is the Bingham number, v [m/s] is the bubble velocity, x [-] is the surface correction factor, y [-] is the rheological correction factor, k [Pa.sⁿ] is the consistency index, n [-] is the power-law index and τ_o [Pa] is the yield stress:

$$C_D = \frac{24x}{Re_{pl}} (1 + yBi_{hb}) \quad (5)$$

$$Re_{pl} = \frac{v^{2-n} d^n \rho_c}{k} \quad Bi_{hb} = \frac{\tau_o}{k(v/d)^n} \quad (6)$$

From the equations above, we calculate the bubble acceleration by:

$$a = \frac{\partial^2 h}{\partial t^2} = \frac{g(\rho_c - \rho_d)}{\rho_d} + \frac{3}{4} \cdot \frac{\rho_c v^2 C_D}{\rho_d d} \quad (7)$$

The equation above works for particles with density different (less or higher) from the fluid density, i.e. gas bubble or solid particles. Therefore,

$$a = \frac{\partial^2 h}{\partial t^2} = \frac{g(\rho_c - \rho_d)}{\rho_d} + \frac{3}{4} \cdot \frac{(\rho_c - \rho_d) \rho_c v^2 C_D}{|\rho_c - \rho_d| \rho_d d} \quad (8)$$

The equation (8) is valid for low or high densities, e.g. gas bubbles or metallic particles.

The bubble diameter is obtained as a function of its displacement, considering that it is a spherical ideal gas bubble in a liquid fluid with constant temperature. Therefore,

$$PV = n_{mm} RT \quad (9)$$

Where V [m³] is the gas volume, P [Pa] is the gas pressure, n_{mm} is the gas molar weight [kg/mol], R [J.K/mol] is the universal gas constant and T [k] is the gas temperature.

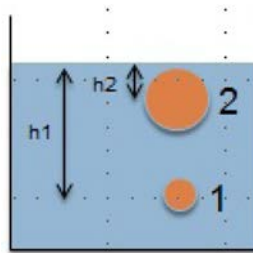


Figure 2. Gas Bubble in different depths.

From eq. (9), and for constant temperature and different depths (Fig. 2).

$$P_1 V_1 = P_2 V_2 = P_n V_n \quad (11)$$

The pressure is related to the bubble displacement by:

$$P_x = P_o + P_h + P_\gamma \quad (12)$$

Where P_o [Pa] is the atmospheric pressure, $P_h = -\rho_c gh$ [Pa] is the hydrostatic pressure, $P_\gamma = 4\gamma/d$ [Pa] is the pressure caused by the surface tension γ [N/m] of the fluid in the gas-liquid interface of the bubble (Adamson et al (1997)), h [m] is the depth, g [m/s²] is the gravity and ρ_c [kg/m³] is the fluid density.

The bubble diameter d [m] is obtained by:

$$d^3 + \frac{4\gamma}{P_o - \rho_c gh} d^2 - \frac{(P_o d_o^3 + \rho_f gh_o d_o^3 + 4\gamma d_o^2)}{P_o - \rho_f gh} = 0 \quad (13)$$

Where h_o [m] is the initial depth of the bubble, and d_o [m] is the initial diameter.

2. NUMERICAL MODEL VALIDATION.

The equation for the bubble acceleration is solved numerically using the second and third order Runge-Kutta method by Bogacki and Shampine. We define the maximum acceptable time step of 0.01[s] to provide stable results.

Figure 3 shows the comparison between the experiments of Raymond F. and J. Rosant (1999) for a gas bubble flowing in a Newtonian fluid and our numerical results. Table 1 shows the rheological properties of the fluid.

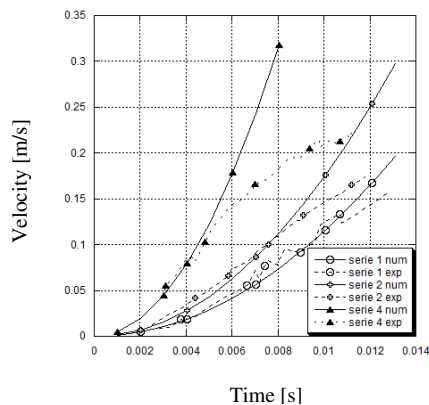


Figure 3: Velocity vs. Time for bubble gas inside a Newtonian fluid: comparison with experiments (Raymond and Rosant, 2006)

Table 1. Rheological properties for Newtonian fluid

| Serie | Viscosity μ [Pa.s] | Density ρ_c [kg/m ³] | Surface tension γ [N/m] |
|-------|------------------------|---------------------------------------|--------------------------------|
| S1 | 0.7 | 1250 | 0.063 |
| S2 | 0.46 | 1245 | 0.063 |
| S4 | 0.16 | 1222 | 0.063 |

Figure 4 shows the comparison between the experiments conducted by Tabuteau et al. (2006) and our numerical results. These results are obtained for a Herschel-Bulkley fluid and rigid spheres (diameter equal to 39.6 [mm]) with different densities, $\rho_{d1} = 1411$ [kg/m³], $\rho_{d3} = 1541$ [kg/m³], $\rho_{d6} = 1736$ [kg/m³].

Table 2. Rheological properties for viscoplastic fluid.

| k [Pa.s ⁿ] | n [-] | τ_c [Pa] | density ρ_c [kg/m ³] |
|------------------------|-------|---------------|---------------------------------------|
| 6 | 0.5 | 7 | 1000 |

Measured at 22°C

Table 2 shows the rheological properties of the fluid.

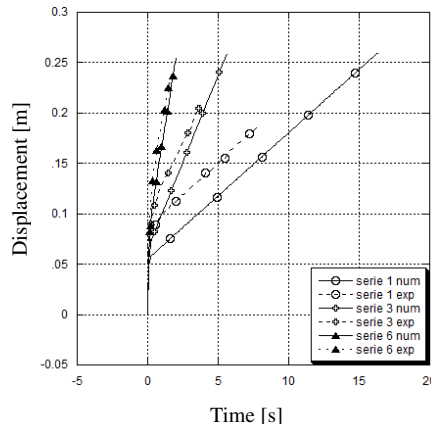


Figure 4: Depth vs. Time for a solid particle inside a viscoplastic fluid: comparison with experiments (Tabuteau et al., 2006)

Figure 5 shows the comparison between the experiments of Neville Dubash (2003) for a gas bubble inside a Viscoplastic fluid and our numerical results. Table 3 shows the rheological properties of the fluid.

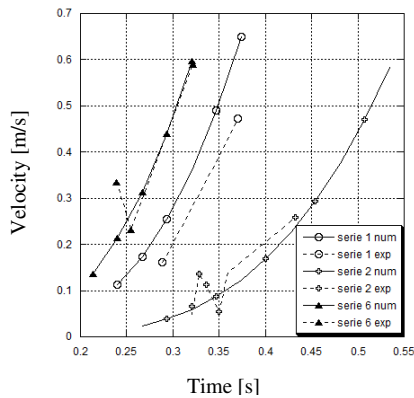


Figure 5: Velocity vs. Time for bubble gas inside a Viscoplastic fluid: comparison with experiments (Neville Dubash, 2003).

Table 3. Rheological properties for Viscoplastic fluid

| Serie | Density ρ_c [kg/m ³] | k [Pa.s ⁿ] | n [-] | τ_c [Pa] |
|-------|---------------------------------------|------------------------|-------|---------------|
| S1 | 1068 | 4.3 | 0.37 | 7 |
| S2 | 1067 | 6.8 | 0.35 | 7 |
| S6 | 1072 | 3.2 | 0.42 | 7 |

Measured at 292.15 K.

It is observed that the results compare well for gas bubbles and rigid spheres in Newtonian and viscoplastic fluids, for lower Reynolds numbers ($Re < 1$), the maximum error calculated was 10%. However, for higher Reynolds it is necessary to use different mathematical models, as expected.

3. INFLUENCE OF SURFACE TENSION FLUID ON THE RESULTS.

In order to calculate the effects of the surface tension, the equation of increased pressure caused by the surface tension $P_\gamma = 4\gamma/d$ was used. Our numerical calculations give results similar to the Adamson and Gast results: the bubble diameter is the main parameter that influences the effect of surface tension: it is important when the bubble is being formed, whereas it is not important when the bubble moves.

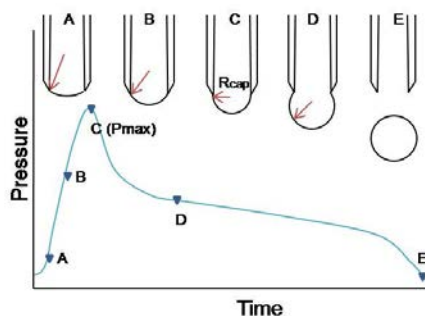


Figure 6: Bubble pressure vs. Time for bubble gas being formed (Adamson and Gast, 1997).

In the Adamson and Gast's results (Fig. 6) the pressure was measured when the bubble is being formed. The pressure increases when the diameter decreases. Fig. 6 show that the pressure is higher in phase C. Tab. 4 shows the rheological properties of the fluid.

Table 4. Rheological properties for Viscoplastic fluid

| Density ρ_c [kg/m ³] | k [Pa.s ⁿ] | n [-] | τ_c [Pa] | Surface tension γ [N/m] |
|--|---------------------------|-------|---------------|-----------------------------------|
| 1250 | 0.7 | 0.42 | 2.2 | 0.465 |

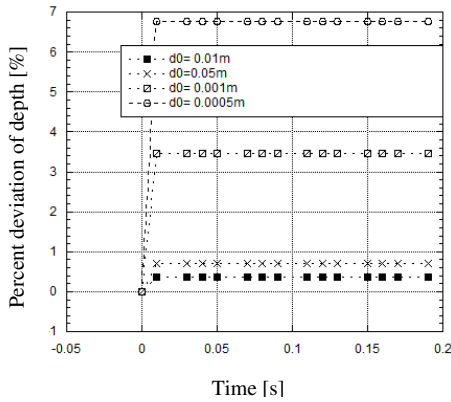


Figure 7: Percent deviation of depth vs. Time for bubble gas inside a Viscoplastic fluid with different surface tension.

Our numerical results (Fig. 7) show larger deviation for lower diameters, the maximum deviation in the example was 7%. The surface tension γ does not directly affect the results.

To calculate the bubble pressure deviation σP_γ [%], the next equation is used.

$$\sigma P_\gamma = \left(1 - \frac{P_o + \rho_c g h}{P_o + \rho_c g h + \frac{4\gamma}{d}} \right) * 100 \tag{14}$$

4. INFLUENCE OF THE BUBBLE MASS ON RESULTS.

The numerical results shown that it is necessary consider the bubble mass on the calculations. The results of the two simulations (Fig. 8 and Fig. 9) with different molar mass, show that the effect of the bubble mass is not negligible.

Table 5. Rheological properties for Newtonian fluid

| Density ρ_c [kg/m ³] | Viscosidade μ [Pa.s] |
|---------------------------------------|--------------------------|
| 1250 | 3 |

Table 5 shows the rheological properties of the fluid.

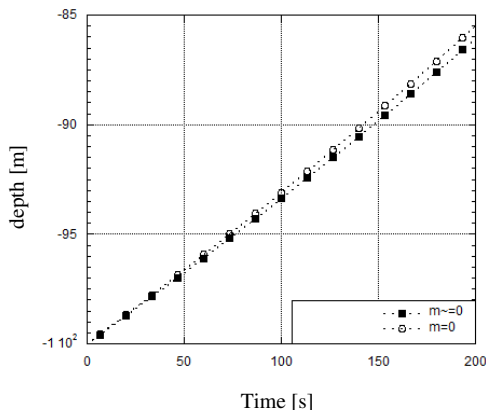


Figure 8: depth vs. Time for bubble gas of butane inside a Newtonian fluid (molar mass of gas: 0.1 [kg/mol]).

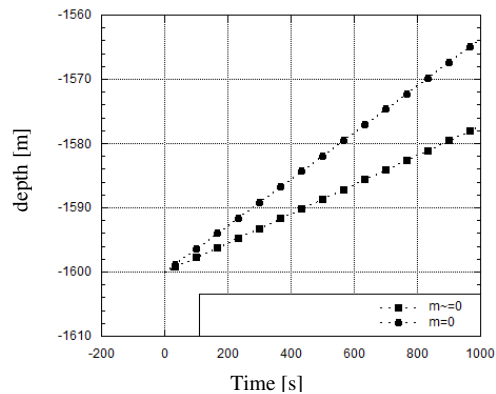


Figure 9: depth vs. Time for bubble gas inside a Newtonian fluid (molar mass of gas: 0.0578 [kg/mol])

The maximum deviation obtained with the simulations (Fig. 8 and Fig. 9) was 38%. The deviations depend on the depth, the molar mass and the bubble initial diameter. Therefore it was not possible to indicate a density of ideal gas that affects the results. In this work we take into account the mass of the bubble in all the calculations.

5. NUMERICAL RESULTS FOR CONSTANT RHEOLOGY

5.1 Results for solid particle

The results (Fig. 10, Fig. 11 and Fig. 12) show the kinematics of solid particles flowing in a viscoplastic fluid. In these simulations the diameter is fixed (3.96 [cm]). It is worth mentioning that in the figures below, the inclination of depth vs. time curve is the velocity of the solid particle. Table 6 shows the rheological properties of the fluid, for the base case.

Table 6. Rheological properties for Viscoplastic fluid

| Density ρ_c [kg/m ³] | k [Pa.s ⁿ] | n [-] | τ_c [Pa] |
|--|------------------------|-------|---------------|
| 1000 | 6 | 0.5 | 7 |

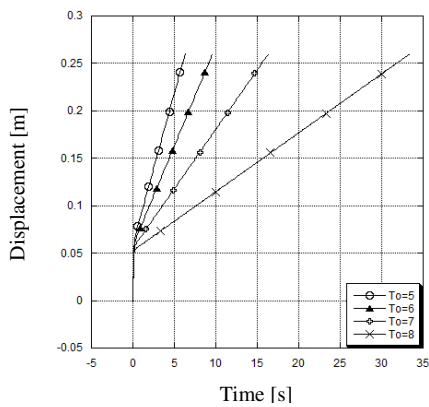


Figure 10: Displacement vs. Time for bubble gas in Viscoplastic fluid: variable yield stress.

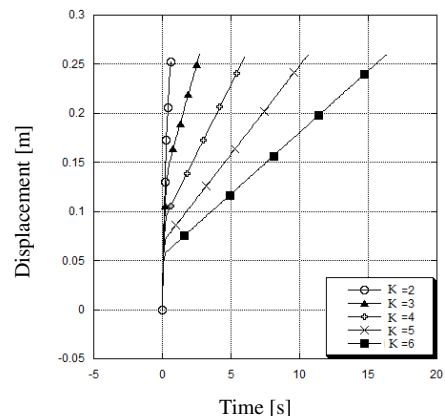


Figure 11: Displacement vs. Time for bubble gas in Viscoplastic fluid: variable consistency index.

The results (Fig. 10 and Fig. 11) show that the increase of the yield stress τ_o and the consistency index k cause a decrease in the terminal velocity. The fluid viscosity increases, then increasing the drag force, which reduces the terminal velocity of the particle (Fig. 10 and Fig. 11).

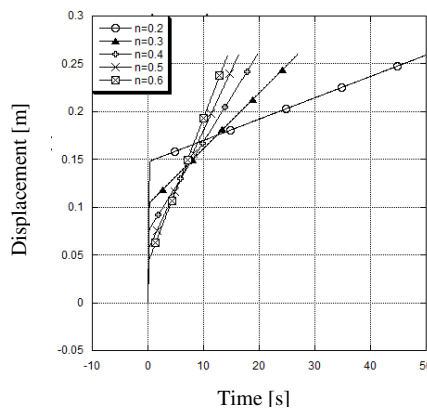


Figure 12: Displacement vs. Time for bubble gas in viscoplastic fluid: variable power-law index.

The results presented in Fig. 12 show that the effect of power-law index n is different. With the increase of the power-law index, the terminal velocity is higher. This behavior is explained by the next equation.

$$\tau = \tau_o + k\dot{\gamma}^n \tag{15}$$

For a shear rate $\dot{\gamma}$ less than 1 [s⁻¹] and an increase of the power-law index n , the shear stress τ decreases and the particle velocity increases. For a shear rate higher than 1 [s⁻¹], the effect is the opposite: the shear stress τ increases causing a decrease in the particle velocity. The particle may accelerate or slow down depending on the shear rate $\dot{\gamma}$. The effect is independent on the power-law index n .

5.2 Results for Gas bubble

The following results show the kinematics of a gas bubble in a viscoplastic. In these simulations the diameter increases according to their depth. Table 7 shows the rheological properties of the fluid, for the base case.

Table 7. Rheological properties for Viscoplastic fluid

| Density ρ_c [kg/m ³] | k [Pa.s ⁿ] | n [-] | τ_c [Pa] |
|--|------------------------|-------|---------------|
| 1072 | 3.2 | 0.42 | 2.2 |

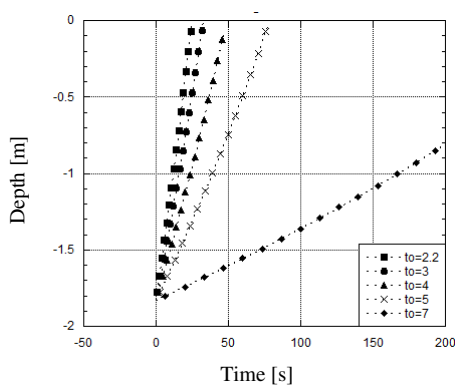


Figure 13: Depth vs. Time for bubble gas inside a Viscoplastic fluid: variable yield stress.

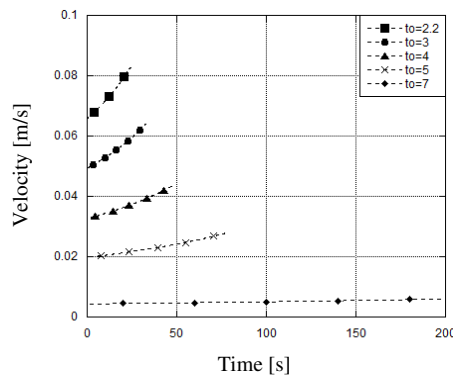


Figure 14: Velocity vs. Time for bubble gas inside a Viscoplastic fluid: variable yield stress.

The Fig. 13 shows that the increase of yield stress τ_o causes a decrease in the velocity bubble. The fluid viscosity increases, then increasing the drag force, which reduces the bubble velocity of the bubble. The Fig. 14 shows the effect of the bubble diameter in the velocity. With the increases of the bubble diameter, the bubble is accelerated. In gas bubble the terminal velocity is not constant.

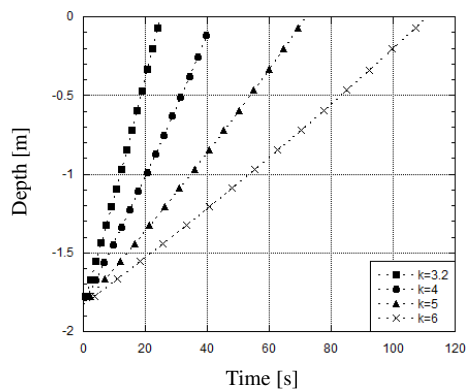


Figure 17: Depth vs. Time for bubble gas inside a Viscoplastic fluid: variable consistency index.

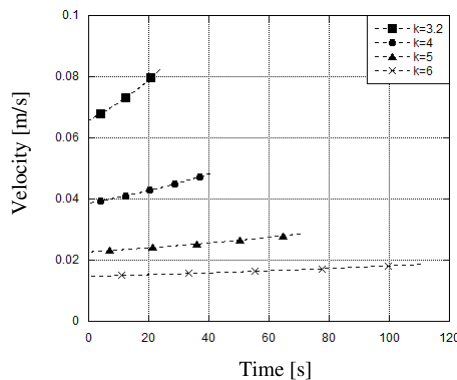


Figure 18: Velocity vs. Time for bubble gas inside a Viscoplastic fluid: variable consistency index.

The results of the Fig. 17 and Fig. 18 are similar to the previous results, the increase of consistency index k causes a decrease in the velocity bubble. In addition, the bubble velocity increases with the bubble diameter.

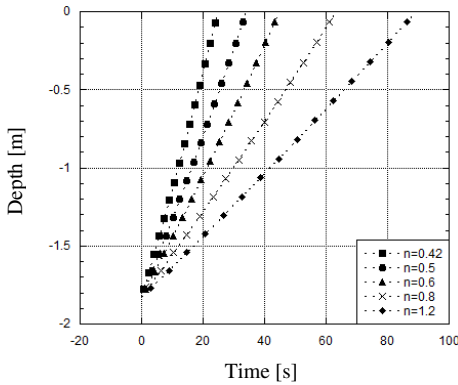


Figure 15: Depth vs. Time for bubble gas inside a Viscoplastic fluid: variable power-law index.

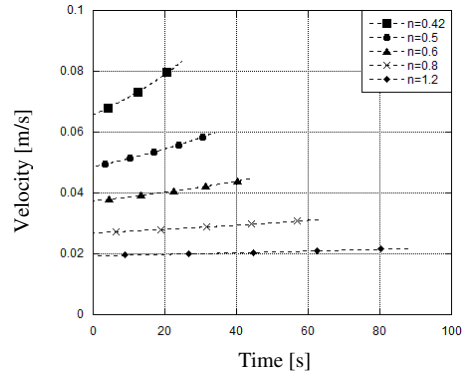


Figure 16: Velocity vs. Time for bubble gas inside a Viscoplastic fluid: variable power-law index.

The results presented in Fig. 15 show that the effect of power-law index n in this case is different. With the increase of the power-law index, the terminal velocity is lower. Its behavior is explained by the next equation.

$$\tau = \tau_o + k\dot{\gamma}^n \tag{15}$$

For a shear rate $\dot{\gamma}$ higher than 1 [s⁻¹] and the increase of the power-law index k , the shear stress τ increases and the particle velocity decreases. The bubble may accelerate or slow down depending on the shear rate $\dot{\gamma}$. The effect is independent on the power-law index n .

6. BEHAVIOR OF THE MATHEMATICAL MODEL FOR VARYING RHEOLOGY.

To analyze the effect of a time dependent rheology, in order to simulate the cement paste behavior, we used the experimental data for real cement pastes, obtained in Pinto et al. (2011) for the consistency index k and the yield stress τ_o :

$$\tau_o = \tau_{o_0} \cdot e^{Ct} \tag{16}$$

$$k = k_o + H \cdot e^{Bt} \tag{17}$$

In the simulations for cement pastes (Fig. 19, Fig. 20 and Fig. 21) the effects of the parameters H , B and C on the bubble kinematic were analyzed. These variables control the behavior of the yield stress and power-law index functions. Table 8 shows the rheological properties of the fluid.

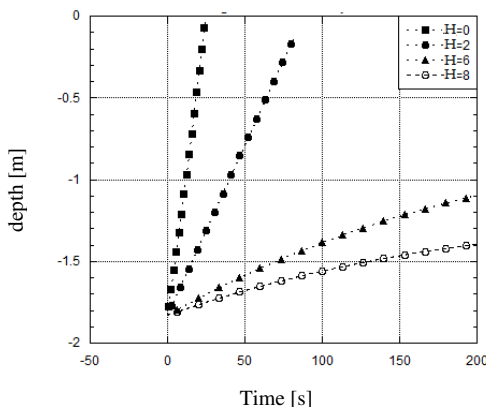


Figure 19: depth vs. Time for bubble gas inside a Viscoplastic fluid of varying rheology: Parameter H .

Table 8. Rheological properties for the initial viscoplastic fluid

| Density ρ_c [kg/m ³] | k_o [Pa.s ⁿ] | n [-] | τ_{o_0} [Pa] |
|--|----------------------------|---------|-------------------|
| 1072 | 3.2 | 0.42 | 2.2 |

Measured at 292.15 K.

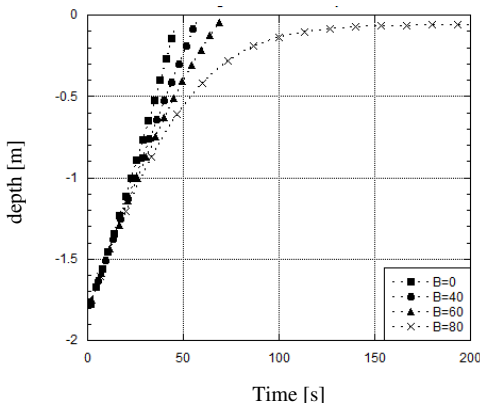


Figure 20: depth vs. Time for bubble gas inside a Viscoplastic fluid of varying rheology: Parameter B.

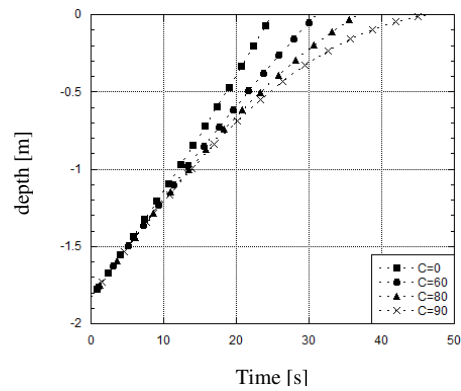


Figure 21: Depth vs. Time for bubble gas inside a Viscoplastic fluid of varying rheology: Parameter C.

The parameters H (Fig. 19) alter quantitatively the results, but the tendency of the curve is not affected. The effect of the parameters B and C is more pronounced (Fig. 20 and Fig. 21). Initially the curve is linear, but with the increase of the B and C parameters, the tendency of the curve changes significantly. Over time the viscosity increases and the bubble velocity decreases until it stops.

8. DRAG COEFFICIENT

Figure 22 shows the drag coefficient results for a gas bubble immersed in a viscoplastic fluid. Table 9 shows the rheological properties of the fluid.

Table 9. Rheological properties for the viscoplastic fluid (Measured at 292.85 K)

| Density ρ_c [kg/m ³] | k_o [Pa.s ⁿ] | n [-] | τ_{o_0} [Pa] |
|--|----------------------------|-------|-------------------|
| 1072 | 3.2 | 0.42 | 2.2 |

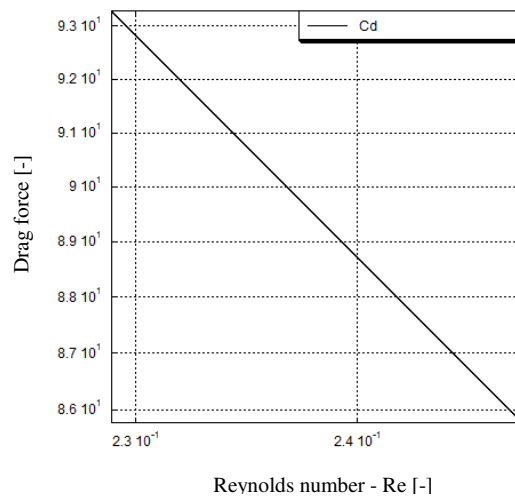


Figure 22: Drag coefficient vs. Reynolds number for bubble gas inside a Viscoplastic fluid.

W. Lopez and M. Naccache
Simplified Mathematical Model for Migration of Gas Bubbles in Viscoplastic.

All the simulations showed the same behavior of the Figure 22, the relationship between the drag force and the Reynolds number is linear, which is similar to the behavior of a gas bubble in Newtonian fluid.

9. CONCLUSIONS

- For low Reynolds numbers ($Re < 3$), the mathematical model works acceptably for inelastic fluids.
- When working with solid and liquid particles with spherical shape condition, the model works acceptably.
- The maximum error of the results is 10%.
- The surface tension of the fluid-gas interface can be neglected
- The mass of the bubble should not be neglected.
- For the case of time dependent rheology, the results are consistent with the expected trend, but experimental studies are needed to validate the results quantitatively.
- For conditions where the Reynolds number is greater than 3, it is necessary to use a more complex model that take into account the shape of the bubble, gas flow and gas diffusion.

10. REFERENCES

- Atapattu D.D, Chhabra R.P. and Uhlherr P.H.T., 1995. *Creeping Sphere Motion in Herschel-Bulkley Fluids: Flow field and drag*. *Journal of Non-Newtonian Fluid Mechanics*. Sydney, Australia.
- Beaulne M. and Mitsoulis E., 1997. *Creeping motion of a sphere in tubes filled with Herschel–Bulkley fluids*. Department of Chemical Engineering, University of Ottawa. Ottawa, Ontario, Canada.
- Bush J. W. M., 2004. *MIT Lecture Notes on Surface Tension*, lecture 3. Massachusetts Institute of Technology, Cambridge, Massachusetts, USA.
- Chhabra R.P., 2007. *Bubbles, Drops, and Particles in Non-Newtonian Fluids*. Indian Institute of Technology, Kanpur, India.
- Dubash, Neville., 2003. *Bubble Propagation through Viscoplastic Fluid. Thesis for the Degree of Master*. The University of British Columbia, Vancouver, Canada.
- Patankar, S. V., 1980, *Numerical Heat Transfer and Fluid Flow*, McGraw-Hill, New York, USA.
- Pinto, G.H.V., Rocha J. M., Campos G., and Martins A. L., 2011. *Metodologia para Avaliação da Migração de Gás após a Cimentação de Poços de Petróleo*, Petrobras. Foz de Iguaçu, PR, Brazil.
- Raymond F. and Rosant J. M., 1999. *A Numerical and Experimental Study of the Terminal Velocity and Shape of Bubble in Viscous Liquids*, Laboratoire de mécanique des fluides, Ecole Centrale de Nantes, Nantes, France.
- Sikorski D, Tabuteau H, Bruyn John, 2009. *Motion and Shape of Bubbles rising through a yield-stress fluid*. Department of Physics and Astronomy, University of Western Ontario, London, Ontario, Canada.
- Tabuteau H., Coussot P. and Bruyn J. R., 2006. *Drag Force on a Sphere in Steady Motion Through a Yield-Stress Fluid*. Department of Physics and Astronomy, University of Western Ontario, London, Ontario, Canada.

11. RESPONSIBILITY NOTICE

The authors are the only responsible for the printed material included in this paper.